Heat and Mass Transfer Research Journal
Vol. 3, No. 2; 2019
Published by CanSRG
http://cansrg.com/journals/hmtrj/

The Effects of Vapor Passage and Structured Evaporator Surfaces on the Performance of Thin Vapor Chambers

Cherng-Yuh Su[1], Wei-Ting Kuo[1], Chen-Kang Huang[2,*]

[1]*Department of Mechanical Engineering, National Taipei University of Technology, Taipei 106, Taiwan*
[2] *Department of BioMechatronics Engineering, National Taiwan University, Taipei 106, Taiwan*

Abstract

For recent mobile devices, vapor chambers are excellent heat dissipation components to avoid hot spots. However, the space for vapor chambers is less and less. In this study, a fabrication process specially designed for thin vapor chambers was proposed. The wick structure was then processed to integrate with vapor passages of various width or structured surface on the evaporation region. Thin vapor chambers with internal vapor core of 0.6 mm in thickness were focused. Vapor passage width of 2, 4, and 6 mm, as well as three structured surfaces on the evaporation region, were fabricated with the thermal performances explored. The thermal performances of the vapor chambers with and without the specific designs for the same thickness of the bulk copper block were compared. It is found that the vapor chamber with vapor passages width of 6 mm and an indented cross on the evaporation region shows the lowest thermal resistance of 0.186 K/W at the heat source supplied power of 100W. The proposed designs are shown to improve the thermal performance of thin vapor chambers.

Keywords: *vapor chamber, flat plate heat pipe, vapor passage, evaporation region.*

Nomenclature

A	Heat transfer area (m^2)
k	Thermal conductivity (W/m K)
L	thickness of the block (m)
Q	heat transfer rate, or heat source supplied power (W)
R	thermal resistance (^oC/ W)
T	temperature (^oC)

Subscripts

c	condensation region
o	outlet
s	surface
th	theoretical
vc	vapor chamber

1. Introduction

Waste heat produced by electronic devices and circuits has to be dissipated to maintain a suitable working temperature and to improve the system reliability. While efforts are paid to lower the heat generated from chips, the electronic cooling is still needed. Good heat dissipation helps the stability of routers, modems, set-top boxes, and mobile devices.

A heat pipe is a heat transfer device that utilizes the evaporation and condensation processes of a working fluid to transfer heat with a small temperature difference between the hot and cold ends. A typical heat pipe is construed by a sealed hollow tube made of copper or aluminum, and a wick inside the tube to return the working fluid from the evaporation to the condensation end. The pipe contains liquid and vapor form of a working fluid. The combination of copper as the container and water as the working fluid is the most common seen in the thermal management industry. The equivalent thermal conductivity of heat pipes can be up to 100,000 W/m K[1].

* Corresponding Author
Submitted: November 25, 2019 Accepted: December 28, 2019

In many applications, round cross-sectional heat pipes are used to transport heat from heat source to heat sink. Vapor chambers (abbreviated VC), also known as flat plate heat pipes, equip similar abilities, but offer a wider and thinner cross-section. VCs are also good heat spreader for chips to reduce hot spots. Like heat pipes, the capillary structure, such as grooves, meshes, or sintered powder, plays an important role on the thermal performance [2].

In recent years, vapor chambers have been studied in many literatures, especially for the applications to electronic cooling [3]. Due to difficulties from experiments and measurement, the experimental results are relatively rare. Theoretical works focused more on the derivation of capillary-driven flows and thermal models [4, 5]. Tang et al. [6] deeply reviewed the recent developments and applications of UTHPs (Ultra Thin Heat Pipe) for electronic thermal management, and the fabrication and heat transfer characteristics with different wick structures.

Huang et al. [7] found that the vapor chamber performance achieved the optimum when the hydraulic diameter ratio of non-wick vapor space to chamber interior was greater than 0.6. Wong and Kuo [8] fabricated specialized flat heat pipes and visualized the operations and found that the wick structure with fine meshes produced greater capillary forces and thinner liquid film thickness. During the evaporation process, the better refill was enabled by using coarse meshes to establish the evaporation region. Water is not the only working fluid in VCs. Lefèvre et al. [9] explored flat plate heat pipes worked with methanol. One or two screen mesh layers and screen meshed covered grooves were used to create the capillary structure. The lowest thermal resistance was exhibited when the wick was made of one single layer copper mesh. Using micro grooves as the wick, the dryout of the evaporator could be limited.

Lips et al. [10] experimentally investigated a copper flat plate heat pipe with a capillary structure made of crossed grooves. The working fluid were methanol and FC72. Crossed grooves performed better than longitudinal grooves. Singh et al. [11] reported that biporous, comparing to monoporous, copper wick structure showed much higher heat transfer coefficient of 83,787 W/m^2 K. The improvement was believed from the improved evaporative heat transfer at wick wall interface and separated liquid and vapor flow pores. Wick structures consisted of layers of different mesh sizes were reported [12]. The 100 + 200 mesh wick, with an upper 100 mesh and a lower 200 mesh woven screen, was sintered on a 3 mm thick copper base plate. The composite wick structure improved the boiling characteristics on the evaporator and led to a very low incipient superheat of 1.3- 4K for methanol and acetone. Weibel et al. [13] explored the wick thickness of sintered powder and its corresponding particle size to find out optimum particle size to achieve a maximum boiling heat transfer coefficient or a minimum thermal resistance. The optimum particle size to have minimum thermal resistance exists when the balance between heat transfer area and vapor flow resistance achieved. The CNT coating was found useful [14] to reduce the incipience superheat of the substrate by 5.6 °C. Unlike most previous researches that have focused on evaporator wicks to reduced thermal resistance and delayed dryout at higher powers, Patankar et al. [15] manipulated the condenser wick to improve lateral heat spreading. A biporous condenser wick was found to get a thicker vapor core, and to decrease the condenser surface peak-to-mean temperature difference by 37%.

Fitting the compact space of the current electronics, the thin heat transfer devices are essential. Thin vapor chambers exhibit the possibility to be sticker-like heat spreaders on electronics to avoid hot spots. Hsieh et al. [16] reported results of thermal resistances for vapor chambers with 10.3 mm in thickness. The spreading (vapor chamber) thermal resistance was around 0.21 K/W, but condenser thermal resistance could be as high as 2.25 K/W. Chen et al. [17] tested vapor chambers

with 3 mm in thickness and created array orthogonal microgrooves to surface functional wicks. For heating power from 20 to 100 Watts, the thermal resistances varied from 0.20 to 0.175 K/W. Yang et al. [18] investigated ulta-thin VC with 1mm in thickness, and achieved thermal resistance of 0.12 K/W with heat power of 20W. Thermal performance of vapor chamber with only 0.28 mm in thickness was reported [19]. The results seemed to imply the higher thermal resistance (4.38 K/W) and low durability. Researchers devote efforts on using various techniques [19] to enhance the performance of thin vapor chambers, including using layers of meshes of multiple sizes, sintered structure with powders of various sizes, and grooved surface on the substrate walls. Some tried to make the movement of vapor and liquid flow smoothly in the compact space without obvious success.

For ultrathin vapor chambers, it is difficult to have the traditional wick-space-wick sandwich structure to allow different paths for liquid and vapor. In this work, to achieve thin vapor chambers with lower thermal resistance, lower equilibrium temperature, and faster thermal response, the vapor passages and structured evaporator surfaces will be explored experimentally.

2. Mathematical Analysis

The vapor chambers designed and fabricated in this work, the corresponding test apparatus, and test procedures will be described in this section.

2.1. Container

In this study, the container of the vapor chamber was constructed by boning the side frame with the top and the bottom substrate. The top and bottom substrate walls of 0.5 mm in thickness, and the side frame of 0.6 mm in thickness were manufactured by CNC. Thereafter, the vapor core is 0.6 mm in thickness for vapor chambers studied in this work. The schematic and the layout of the wick structure are shown in Figure 1.

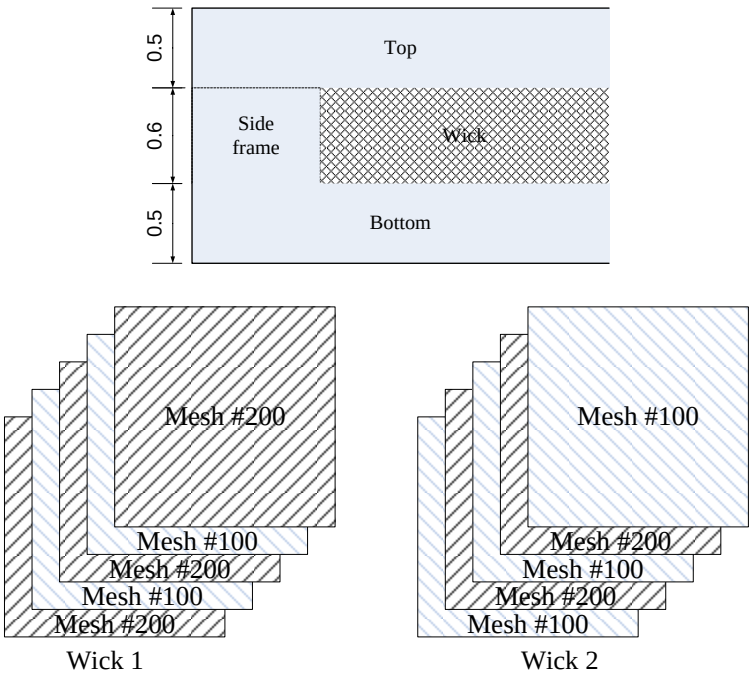

Figure 1. Schematic of the assembly of the 0.5 mm substrate walls and 0.6 mm side frame; Construction schematic of the wick structure 1 and 2 established by layers of copper meshes.

2.2. Wick Structure

The wick structure was established using 5 layers of copper meshes with different mesh numbers. The specifications of the copper meshes can be found in Table 1. Two kinds of wick structure were fabricated and tested in this work. In order to avoid middle mesh collapsing in adjunct layers after the bonding process, the subsequent mesh was rotated by 45o. For wick structure 1, the structure was constructed with copper screen meshes in the order of #200/ 100/ 200/ 100/ 200. For wick structure 2, the #100/ 200/ 100/ 200/ 100 arrangement was used. The constructions of the two wick structures can also be found in Figure 1. The copper meshes were bonded to form the wick structures. The shrinking in thickness and their final thickness will be discussed in Section 3.

Table 1. Specifications of copper meshes used in this study.

Mesh number	*#100*	*#200*
Thickness (mm)	0.22	0.11
Wire diameter (mm)	0.114	0.051
Aperture (mm)	0.146	0.076

In this study, various water filling amount was tested for optimal performance, and the filling loading ratio [18] of 125% was selected for all VCs.

2.2. Vapor Passages with Various Width

After the wick structure was fabricated, they were trimmed for the patterns with various vapor passage widths. The diagonal oriented vapor passages were 2, 4, and 6 mm in width. 3 wick structures with 2, 4, or 6 mm vapor passage width are shown in Figure 2. These trimmed wicks were assembled to vapor chambers for tests, as shown in Figure 3. The outer dimensions of the finished thin vapor chamber are 90 mm in length, 55 mm in width, and 1.6 mm in thickness. On the other hand, those are fabricated with same fabrication process using wick structure without vapor passages are defined as the regular VC in this study.

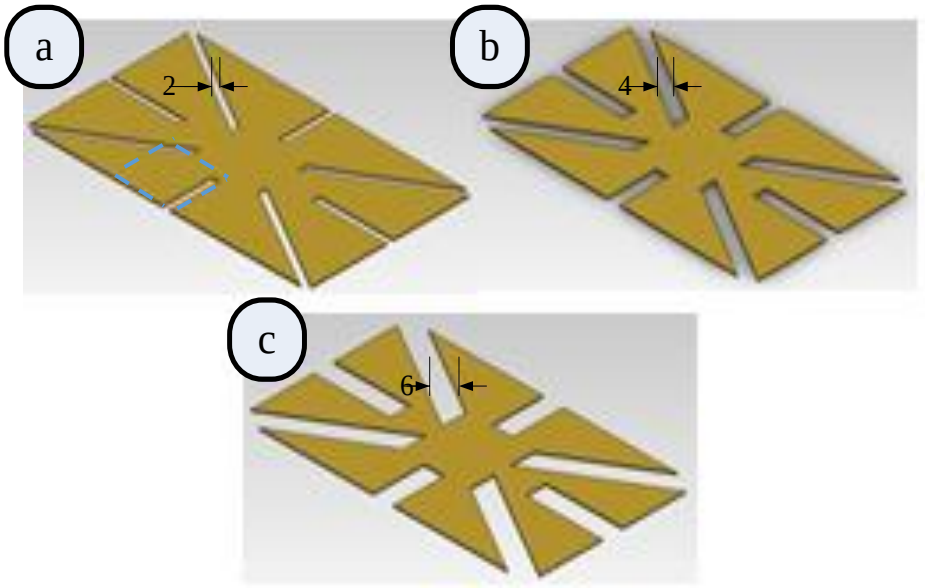

Figure 2. Schematic of the wick structures with vapor passages of (a) 2 mm, (b) 4 mm, and (c) 6 mm in width.

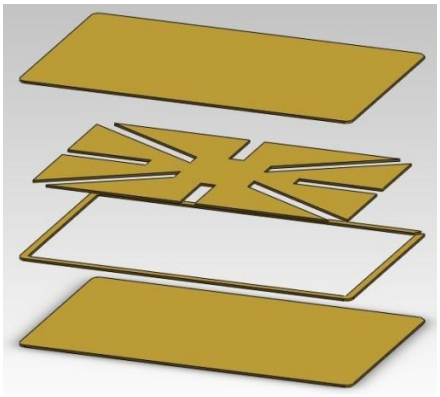

Figure 3. Explosion view of the vapor chamber proposed in the study.

2.3. Structured Surface on the Evaporation Region

Referring the literature [14], the structured surfaces were fabricated on copper mesh to integrate with the wick. Three graphite molds for surfaced surfaces were made. On a trimmed #100 mesh, the structure surfaces on the evaporation region were sintered with #150 to #320 mesh copper powders at 850 ^{o}C for 90 minutes. The sintering process ensured no voids occurring between the mesh and powders, but may increase the flow resistance. This layer of mesh was then bonded with the other four layers to construct the wick structure with both the vapor passages and structured surfaces on the evaporation region (Figure 4).

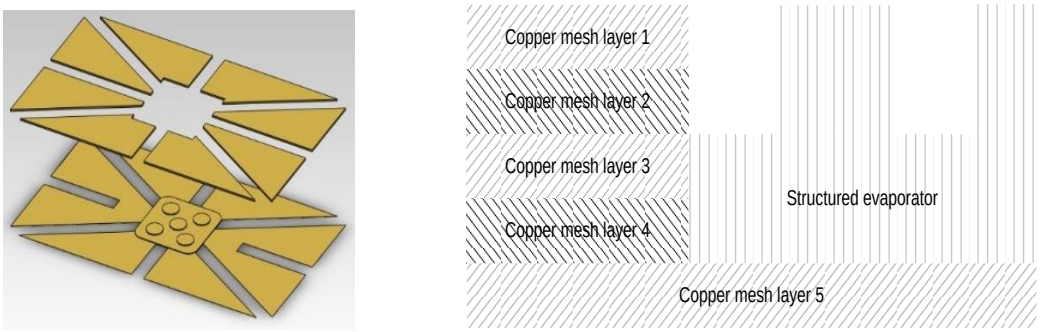

(a) (b)

Figure 4. Schematic of (a) the assembly of the wick structure with vapor passages and the structured evaporator surface, (b) the cross section of the junction of the wick structure and the evaporator.

Three patterns of the structured surfaces were explored. A schematic of the structured surfaces with short extruded pillars (4 mm in diameter), an extruded cross (4 mm in width, and 12 mm in length), or an indented cross (4 mm in width) on the evaporation region was shown in Figure 5. For all three structures, the base and the extruded parts are about 2 layers of copper meshes in thickness. For VCs working at 50 to 100 ^{o}C, the capillary limitation dominates. When the supplied heat is enough, it is expected that all side walls and top surfaces can be the evaporation area. Consequently, side wall area can be the extra. It is expected that the structured surfaces increase the evaporation area, enhances the working fluid diffusion, and avoid the vapor block in the evaporation region.

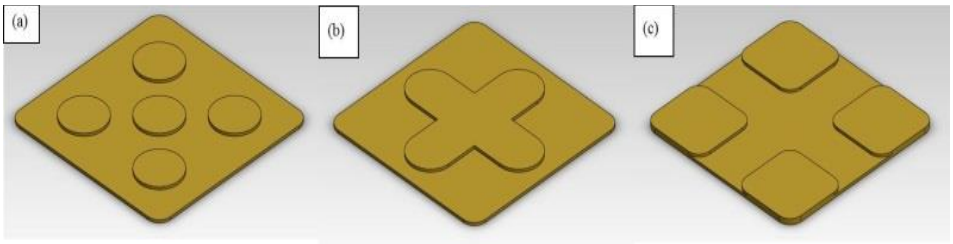

Figure 5. Schematic of the sturctured surfaces with (a) extruded pillars, (b) an extruded cross, or (c) an indented cross on the evaporation region.

2.4. Thermal Resistance Measurement

A thermal resistance measurement apparatus (LW-9091, Longwin, Taiwan) was utilized. A 16 mm by 16 mm area was used to transfer energy into the vapor chamber from the bottom. The heat source supplied power varied from 10, 20, 40, 60, 80, to 100 W. A water jacket was attached on the other side of the vapor chamber for the heat removal, and the heat removal area was 60 mm by 50 mm. According to manufacturer's experience, the cooling water mass flow rate through the condensation water jacket was set as 2.5 g/s. To achieve a vapor chamber average temperature, which is the average between evaporation and condensation regions, close to the actual applications, the flow rates were chosen. The mass flow rate of 2.5 g/s was controlled by a precision flow regulator. The cooling water was supplied by a refrigeration circulator with a temperature setting at 25 ^{o}C. Shallow grooves were machined on the bottom of the water jacket for the installation of six thermocouple wires. The temperature measuring points are shown in Figure 6, where T1and T6 are located above the wick structure, T2 and T5 are located above the vapor passages, and T3 and T4 are located above the edge of the heater. Thermal grease was applied on both sides of the test vapor chamber to reduce the contact resistance. The heat source surface temperature can be extrapolated by using the empirical equation given by the manufacturer of the test apparatus.

$$\Delta Q = \frac{kA}{L} \cdot \Delta T = 2.464 \cdot \left(T_L - T_U\right) \tag{1}$$

where k is the conductivity of heating element, A is the calculation heat transfer area, L is the calculation heat transfer length, and T_L and T_U are the corresponding readings on the apparatus. The displacement of the heat source, water jacket, and temperature measuring points can be found in Figure 6(a). A load cell was installed between the down-pressing mechanism and the test assembly. Based on the load cell reading, the same downward force of 20 kg-f could be kept.

The vapor chamber thermal resistance is calculated from Eq. (2).

$$R_{vc} = \frac{T_s - T_{vc,t}}{\dot{Q}} \tag{2}$$

where R_{vc} is the vapor chamber thermal resistance, T_{vc}, t is the estimated VC top surface temperature (average of T3 and T4 in Figure 6(a)), Ts is heat source surface temperature which is extrapolated from internal readings of the heat source (LW-9091, Longwin, Taiwan), and Q is the heat source supplied power (LW-9091, Longwin, Taiwan). The heat source surface temperature, and the heat source supplied power were the two measurements in the experimental investigation. According to the specifications of the test apparatus, the uncertainty for the temperature is ±0.5%. Besides, the heat source supplied power was derived from the two RTD readings on the heating pod. It is estimated that the uncertainty for the supplied power is ±5%.

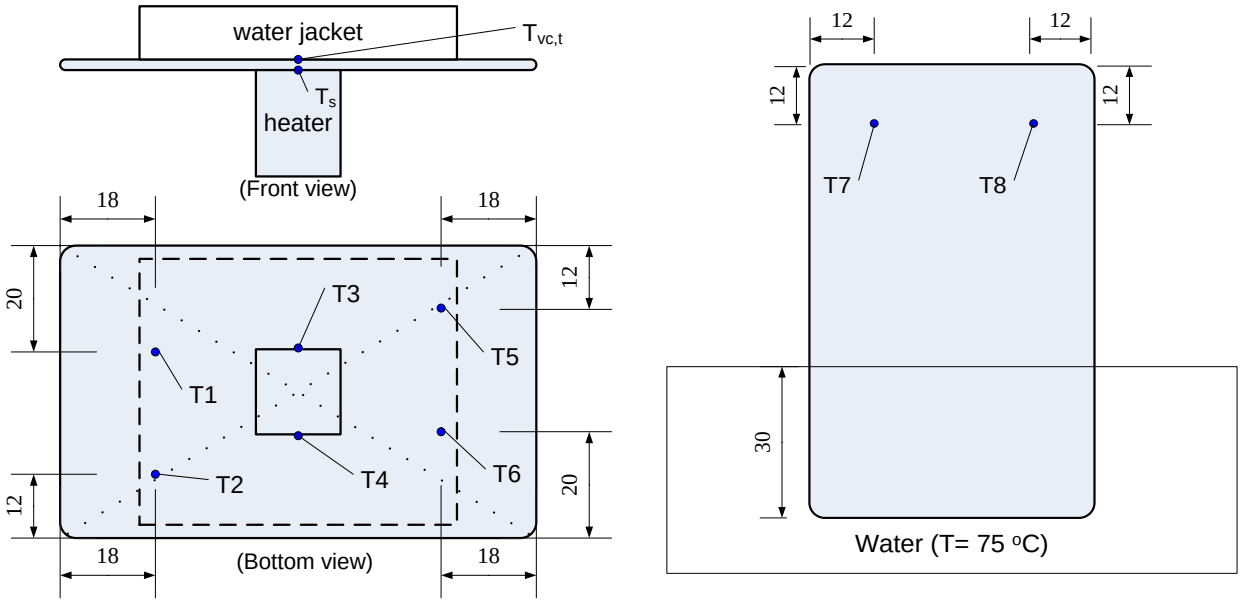

Figure 6. The test apparatus for the (a) thermal resistance and (b) thermal response.

2.5. Thermal Response Measurement

While thermal resistance represents how good the device spreads heat at a temperature difference, it is also expected to have the other index to show how fast the device transports energy. The setup for thermal resistance is capable of measuring the response time. However, this configuration is heated from the center with a shorter length to measure temperature variation. Referring similar apparatus in the literature [19], the thermal response was measured using the designed apparatus and the following procedures. In order to have a longer distance to observe the response from the temperature variations, the second test configuration was designed. The test VC is heated from one side of the VC by soaking into a pool of hot water with a constant depth of 30 mm. Two thermocouple couples are attached on the VC surface and the locations are 12 mm and 12 mm inside the corners of the VC. From the thermocouple readings, the surface temperature variations on the opposite side could be recorded. If the temperature variation was less than 0.4 ºC for at least 5 minutes, it was defined that the steady state was achieved [16]. It would be expected that a vapor chamber is good at thermal response if the steady state can be achieved with less time. A pool of water which was maintained at 75 ºC was used as the heat source. Temperature variation histories from the average of the two points, which belonged to the vapor passage region, on the vapor chamber surface were recorded for analysis. The thermal response measuring apparatus is shown in Figure 6(b).

3. Experimental Methods

3.1. Wick Construction Determination

For the two wick structures fabricated in this study, key parameters are shown in Table 2. It was estimated that the wick structure thickness would shrunk for 15 to 25% after the bonding process. After actual bonding and cutting, it was observed that the thickness of the wick 1 and 2 was eventually 0.55 mm and 0.59 mm, respectively. From Table 1, comparing to the #100 mesh, #200 mesh itself is less in thickness. Consequently, the wick 1 was thinner due to three #200 meshes

constructing the wick structure. On the contrary, three #100 meshes were used in wick 2 leading to a thicker wick. The wick 2 was able to have a wick structure closer to the specification of 0.6 mm in thickness.

Table 2. Specifications of the wick structures fabricated in this study.

Wick structure specifications	*Wick 1*	*Wick 2*
Ideal vapor core height (mm)	0.6	0.6
Actual vapor core height (mm)	0.55	0.59
Wick thickness before bonding (mm)	0.67	0.74
Thin VC thickness (mm)	1.6	1.6

The optical images for structures and bonding of wick 1 and wick 2 are shown in Figure 7. Comparing (b) and (d) in Figure 7, it can be found that the interface void in wick 1 is more obvious than that in wick 2. The wick 1 could be broken down easily. The wick 2 exhibits a better diffusion bonding with little gap. Therefore, parameters of wick 2 were selected to construct subsequent wick structures in this work.

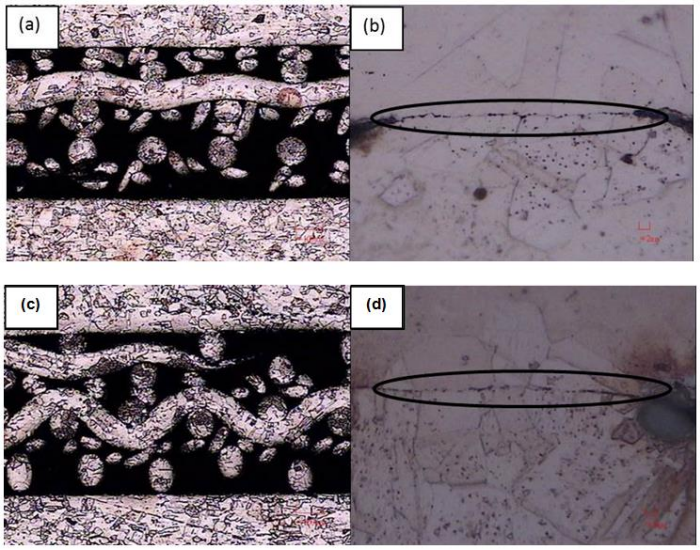

Figure 7. Optical microscope image of wick structure 1 ((a) 5X (b) 1000X) and wick structure 2 ((c) 5X (d) 1000X).

3.2. Reliability of the Wick Structure

From the vapor chamber manufacturers' point of view, less VC thickness variation represents better manufacturing and higher product reliability. The reliability tests were performed to be maintained at 145 ºC for 4 hours. The temperature of 145 ºC produces a double temperature difference on a VC, comparing to the usual usage on consumer electronics. In Figure 8, eleven measuring points were measured on the surface. According to the measurement, the variation of vapor chamber height is less than 0.02 mm. It shows that the current configuration and manufacturing procedures are reliable and solid.

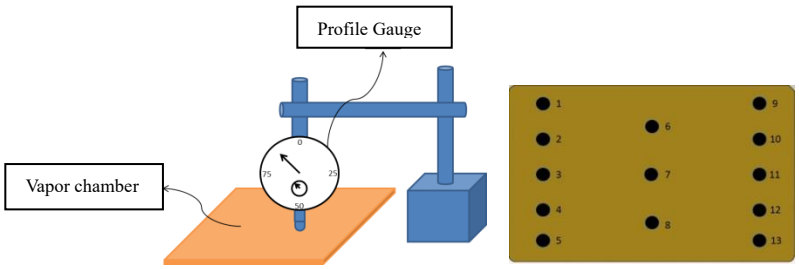

Figure 8. Schematic of test method and locations (marked as 1 to 13) for the vapor chamber thickness.

3.3. Thermal Performance of Thin Vapor Chambers

3.3.1. Thermal Response Tests

To explore the thermal response of vapor chambers, one part was tested by contacting with a high temperature source, and the other was exposed in the air. Two thermocouples were attached on the part exposed in the air. During tests, readings from the two thermocouples were recorded. The temperature differences between the average temperatures of test points and the heat source were used to evaluate the thermal response of the vapor chamber. The test apparatus for the thermal response is shown in Figure 6(b). Experimental set-up in Figure6 was based on the design in the literature [19]. The traditional measurement may not be able to fully response for the new VC design with evaporation region located at the center of the VC. Since the thermal response tests were to observe the transient period before the equilibrium achieved, using an IR thermal video recorder may a better way to explore the VCs with special designs at the center.

A bulk copper block of the same size, a thin VC with the regular design, thin VCs with vapor passage width of 2, 4, or 6 mm, and the VCs with 6 mm vapor passages and the structured surfaces with extruded pillars, an extruded cross, or an indented cross on evaporation region were tested. Using a pool of water at 75 ^{o}C as the heat source, the temperature differences between the test points and the heat source for a time elapsed of 90 seconds were recorded. The environmental temperature was set at 28 ^{o}C.

Figure 9 shows the thermal response comparison. For all cases, the temperature difference decreases initially and becomes steady at a relatively unchanged temperature difference. When the temperature difference becomes steady, it is believed that equilibrium is achieved. It is found that wider vapor passages lead to shorter time to achieve equilibrium and a lower final temperature difference. It is believed that the vapor core is not high enough to create smooth vapor and liquid flows inside the vapor chamber with the regular design causing a long equilibrium time. Between VC with special vapor passage designs, regular VC, and bulk copper block, the VC with vapor passage width of 6 mm is the most responsive one. It takes 25 seconds to achieve the temperature difference of less than 10 ^{o}C. Besides, it takes 55 seconds to achieve the equilibrium temperature of 68.7 ^{o}C. Comparing to the results, it can be found that wider vapor passages lead to shorter time to achieve equilibrium. However, the width of the vapor passages shows little effects on the equilibrium temperature.

The time achieving equilibrium and equilibrium temperature can be used to evaluate the VC performance. Shorter time achieving equilibrium represents better spreading of heat. The vapor chamber with vapor passage width of 6 mm is the best in the thermal response, which is faster than the bulk copper block and the regular vapor chamber.

While most working liquid movement occurs in the wick structure, the only interfaces between vapor and liquid flow are the side walls of the passages, which do not vary with the passage width. Consequently, the improvement from wider passages is believed from the decrease flow resistance of the vapor flow in the passages. Vapor passages do somehow solve the common shortcomings in thin vapor chambers. However, wider passages reduce more wick structure. It is believed that the optimum ratio between wick and passages is a function of vapor core height. More efforts should be paid to examine the hypothesis.

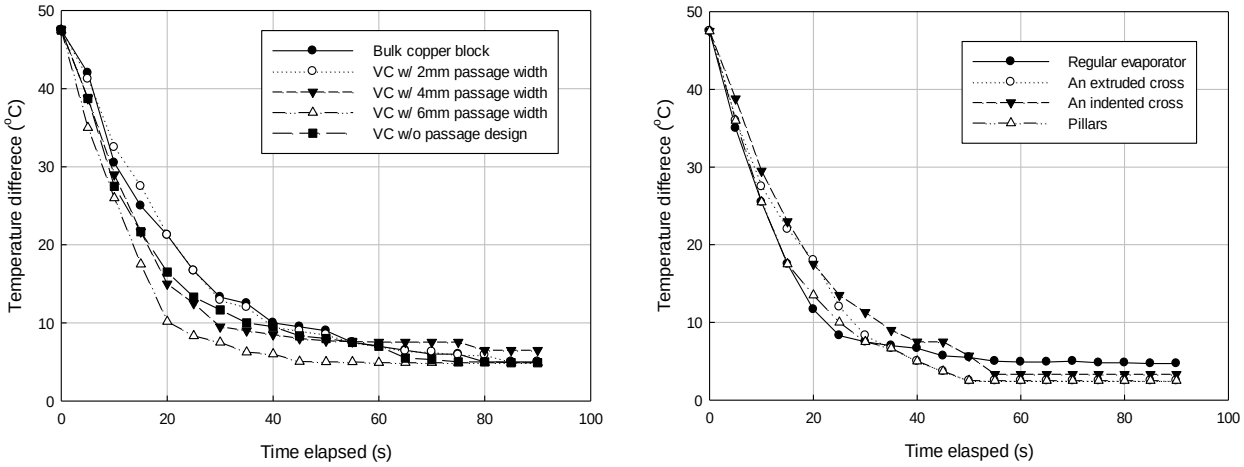

Figure 9. Thermal response results of (a) the bulk copper block, the VCs without vapor passages, the VC with vapor passages with 2, 4, or 6 mm in width, (b) the VCs with 6 mm vapor passages and structured surfaces of extruded pillars, an extruded cross, or an indented cross on the evaporation region.

Since the VC with vapor passage width of 6 mm exhibited the best thermal response, the wick structure with vapor passages of 6 mm in width were then integrated with the structured surface in the evaporation region to study the effects on the VC performance. Comparing the VCs with both vapor passages of 6 mm in width and structured evaporator surfaces, the thermal response sequence of the structured surface is no structured surface, extruded pillars, an extruded cross, and an indented cross, from fast to slow. While the thin VC with structured evaporator surfaces are not more thermal responsive than the thin VC with vapor passage of 6 mm in width, the structured evaporator surfaces do decrease the equilibrium temperature differences.

3.3.2. The Effects of Vapor Passage Width on the Thermal Resistances

The maximum heat transfer rate and thermal resistance are commonly used to evaluate VCs. Higher maximum heat transfer rate and lower thermal resistance are two indicators of good VCs. Experimental results of various vapor passage width are plotted in Figure 10.

When the heat transfer rate increases, the thermal resistance usually drops. This trend is related to the fluid properties, which are functions of temperature. When increasing the heat source supplied power, it can be found that thermal resistance decreased and tended to steady for higher supplied power. From literatures [4, 7, 9, 20], heat transfer drops when the vapor space decreases. Less vapor space limits the flow of working fluids, leading to higher flow resistance. The design proposed in this work mainly focus on separated flow between vapor and liquid. Taking experimental data from supplied power of 100W as an example, thermal resistances of VCs with vapor passage width of 2, 4, and 6 mm are 0.241, 0.213, and 0.194 K/W, respectively. These were

all lower than the thermal resistance (0.284 K/W) of the VC without vapor passages. Results show that the proposed vapor passage design solves the high thermal resistance problems for common thin VCs.

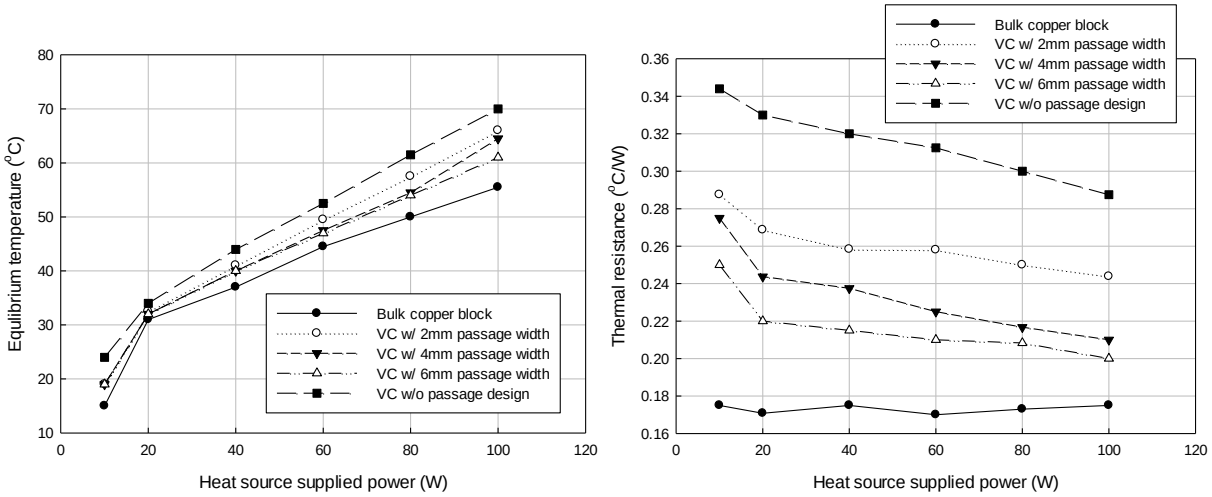

(a) (b)

Figure 10. (a) The equilibrium temperatures and (b) thermal resistances of the bulk copper block, the VC without passage design, and thin VCs with vapor passages of 2, 4, and 6 mm in width.

Comparing to the bulk copper block, the thermal resistance of the thin VCs with 6 mm vapor passages is still higher by 0.21 K/W. It seems to imply that the passages can be wider. Currently, 6 mm passages approximately occupy 30% of the total substrate area. The capillary force in the wick should be balanced with the flow resistance of liquid and vapor phase. The additional design of 6 mm passages decreases the wick area and the total capillary force. However, less wick area also leads to less flow resistance. These changes move the operation point to be a new location. However, the visualizable VCs are still not available to clarify the internal processes. It is also not clear that the flow inside is filmwise or dropwise. The above description is the commonly accepted hypothesis.

For the optimal vapor passage width, more analytical analysis, experiments, and manufacturing feasibility and durability should be required to be considered comprehensively. Although current thin vapor chambers still exhibit resistance higher then bulk copper block, the overall weight of thin vapor chambers are about 1/3 lighter. When the vapor passages are optimized, the thin vapor chambers are still highly expected.

3.3.3. The Effects of Structured Evaporation Surfaces on the Thermal Resistances

Experimental results of various structured surfaces are plotted in Figure 11. For lower supplied power, 10 to 80 W, the structured evaporator surfaces do not show any advantages. The thermal resistances are higher than those from VC's without the structured vapor surface. Only when the supplied power is higher than 100 W, the structured surface of an indented cross exhibited a lower thermal resistance. The VC with vapor passage width of 6 mm shows a heat source surface temperature of about 61 ºC when supplied power is 100 W. The heat source surface temperature is the second lowest in this study. For those cases with higher temperature tolerance, the applicable situation can be more than 100 W.

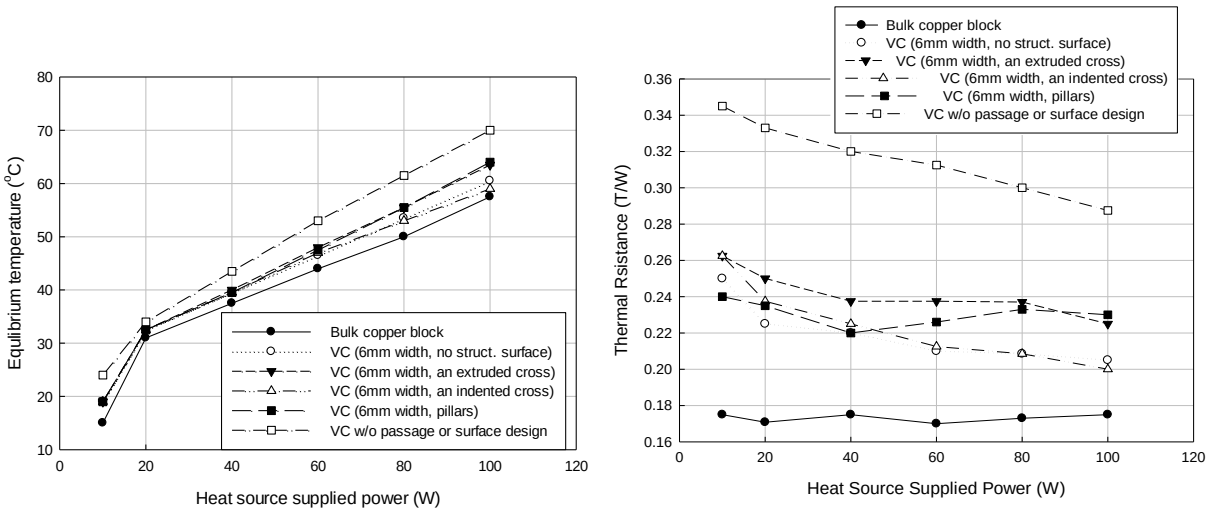

(a) (b)

Figure 11. (a) The equilibrium temperatures and (b) thermal resistances of the bulk copper block, the VC with vapor passages of 6 mm in width, the VC with vapor passages and short extruded pillars, an extruded cross, or an indented cross on the evaporation region, and the VC without vapor passages or structure surface.

According to the thermal resistance, the performance sequence of the structured surface from good to poor is an indented cross, no structured surface, extruded pillars and an extruded cross. During the sintering process, some pressure should be applied to keep the structured surface stick on the copper mesh to avoid unnecessary contact resistance. Although the integration of structured surfaces might not reduce thermal resistance effectively, the structured surfaces lowered the equilibrium temperature by 5 ºC. Current results seem not to justify the effects of patterns of the structured surface on the VC performance. A sintered structure with finer powders leads to a finer porous structure and a higher flow resistance. On the other hand, the structure with coarser powders exhibits lower flow resistance but weaker strength. In this study, finer powders were used to construct the structured evaporator surface increasing the liquid flow resistance. Structured surfaces with an extruded cross or several extruded pillars reduce the empty space above the evaporator further increasing the vapor flow resistance. These are speculated as the reason that the structured surface with an indented cross shows the best performance, since there is less structure constructing from fine powders and spacious empty space above the evaporator.

The equivalent thermal resistance of bulk copper block can be derived as follows.

$$R_{th} = \frac{\Delta T}{\dot{Q}} = \frac{L}{kA} \tag{3}$$

where T is the temperature difference between the top and the bottom of the block, Q is the heat source supplied power, L is the thickness of the block (m), k is the thermal conductivity of the block (W/ m K), and A is the heat transfer area (m^2). For the test in this study, the theoretical thermal resistance [21] of the bulk copper block is about 0.016 W/K. It implies that the contact resistance for the heating and cooling area can be estimated as 0.154 W/K. High evaporator and condensation thermal resistance were reported in the literature [16]. If the estimated contact resistance is deducted from the measurement in Figure 10 and 11, the thermal resistances of VCs themselves are between 0.051 to 0.191, which are on the same order of results in the literature [18].

4. Conclusions

By constructing the wick with vapor passages and structured evaporator surface, a new design was

established to fabricate thin vapor chambers. Wick structures created by layers of copper meshes were fabricated, and the reliability was tested. Thermal resistance and thermal response were tested to evaluate the thin vapor chamber performance.

The wick structures constructed by layers of copper meshes were tested at 145 ºC for 4 hours. The thickness variation was less than 0.02 mm. The good reliability is verified.

The idea of independent vapor passages was successfully integrated into thin vapor chambers and reduced the thermal resistance. From the thermal response results, the thin vapor chamber with vapor passages of 6 mm in width and structured evaporator surface showed the best thermal response. It showed no improvement on the time to achieve equilibrium, but the VCs with special designs showed lower equilibrium temperatures. While only the structured surface of an indented cross was able to further decrease the thermal resistance with a heating power of 100 W, the structured surfaces did show lower equilibrium temperatures.

The VC with vapor passages of 6 mm in width and the structured evaporator surface of an indented cross showed the best performance, achieving a thermal resistance of 0.186 K/W with a heating power of 100 W. Two key parameters are concluded that the vapor passages reduce the thermal response as well as thermal resistance, and the structured surfaces reduce the equilibrium temperature.

Acknowledgments

This work was supported by Ministry of Science and Technology (MOST) of Taiwan (MOST 108-2221-E-002-047).

References

[1] D. R. R. McGlen and P. Kew, Heat pipes: Theory, Design and Applications (6th ed.), Oxford, Butterworth-Heinemann, 2013.

[2] F. Lefèvre, S. Lips, R. Rullière, J. Conrardy, M. Raynaud, and J. Bonjour, Flat plate heat pipes: from observations to the modeling of the capillary structure, Frontiers in Heat Pipes, vol 3, pp. 1- 9, 2012.

[3] L. Vasiliev, Micro and miniature heat pipes-Electronic component coolers, Applied Thermal Engineering, vol 28(4), pp. 266-273, 2008.

[4] S. J. Kim, J. K. Seo, and K. H. Do, Analytical and experimental investigation on the operational characteristics and the thermal optimization of a miniature heat pipe with a grooved wick structure, International Journal of Heat and Mass Transfer, vol 46 (11), pp. 2051-2063, 2003.

[5] F. Lefèvre, R. Rullière, G. Pandraud and M. Lallemand, Prediction of the temperature field in flat plate heat pipes with micro-grooves-Experimental validation, International Journal of Heat and Mass Transfer, vol 51(15), pp. 4083-4094, 2008.

[6] H. Tang, Y. Tang, Z. Wan, J. Li, W. Yuan, L. Lu, Y. Li and K. Tang, Review of applications and developments of ultra-thin micro heat pipes for electronic cooling, Applied Energy, vol 223, pp. 383-400, 2018.

[7] C. K. Huang, C. Y. Su and K. Y. Lee, The Effects of Vapor Space Height on the Vapor Chamber Performance, Experimental Heat Transfer, vol 25(1), pp. 1-11, 2012.

[8] S.-C. Wong and Y.-H. Kao, Visualization and performance measurement of operating mesh-wicked heat pipes, International Journal of Heat and Mass Transfer, vol 51(17), pp. 4249-4259, 2008.

[9] F. Lefèvre, J. Conrardy, M. Raynaud, and J. Bonjour, Experimental investigations of flat plate heat pipes

with screen meshes or grooves covered with screen meshes as capillary structure, Applied Thermal Engineering, vol 37, pp. 95-102, 2012.

[10] S. Lips, F. Lefèvre and J. Bonjour, Thermohydraulic study of a flat plate heat pipe by means of confocal microscopy: application to a 2D capillary structure, Journal of Heat Transfer, vol 132(11), pp. 112901-9, 2010.

[11] R. Singh, A. Akbarzadeh and M. Mochizuki, Effect of wick characteristics on the thermal performance of the miniature loop heat pipe, Journal of Heat Transfer, vol 131(8), pp. 08260 1-10, 2009.

[12] S. -C. Wong, Y. -C. Lin and J. -H. Liou, Visualization and evaporator resistance measurement in heat pipes charged with water, methanol or acetone, International Journal of Thermal Sciences, vol 52, pp. 154-160, 2012.

[13] J. A. Weibel, S. V. Garimella and M. T. North, Characterization of evaporation and boiling from sintered powder wicks fed by capillary action, International Journal of Heat and Mass Transfer, vol 53(19), pp. 4204-4215, 2010.

[14] J. A. Weibel, J. A., A. S. Kousalya, T. S. Fisher and S. V. Garimella, Characterization and nanostructured enhancement of boiling incipience in capillary-fed, ultra-thin sintered powder wicks, Proceedings of 13th IEEE Intersociety Conference on Thermal and Thermomechanical Phenomena in Electronic Systems (ITherm), pp. 119-129, 2012.

[15] G. Patankar, J. A. Weibel and S. V. Garimella, Patterning the condenser-side wick in ultra-thin vapor chamber heat spreaders to improve skin temperature uniformity of mobile devices, International Journal of Heat and Mass Transfer vol 101, pp. 927-936, 2016.

[16] S. S. Hsieh, R. Y. Lee, J. C. Shyu and S.W. Chen, Thermal performance of flat vapor chamber heat spreader, Energy Conversion and Management, vol 29(6), 2008.

[17] G. Chen, Y. Tang, Z. Wan, G. Zhong, H. Tang and J. Zeng, Heat transfer characteristic of an ultra-thin flat plate heat pipe with surface functional wicks for cooling electronics, International Communications in Heat and Mass Transfer, vol 100, pp. 12-19, 2019

[18] K. S. Yang, C. W. Tu, W. H. Zhang, C. T. Yeh and C. C. Wang, A novel oxidized composite braided wires wick structure applicable for ultra-thin flattened heat pipes, International Communications in Heat and Mass Transfer, vol 88, pp. 84-90, 2017.

[19] S. Xu, R. J. Lewis, L. A. Liew, Y. C. Lee and R. Yang, Development of Ultra-Thin Thermal Ground Planes by Using Stainless-Steel Mesh as Wicking Structure, Journal of Microelectromechanical systems, vol 25(5), pp. 842- 844, 2016

[20] D. Khrustalev and A. Faghri, Thermal characteristics of conventional and flat miniature axially grooved heat pipes, Journal of Heat transfer, vol 117(4), pp. 1048-1054, 1995.

[21] J. Velardo, R. Singh and A. Date, An Investigation into the Effective Thermal Conductivity of Vapour Chamber Heat Spreaders, Energy Procedia, vol 110, pp. 256-261, 2017.

Biographical information

C.Y. Su currently serves as Professor of the Department of Mechanical Engineering at National Taipei University of Technology (Taipei TECH), Taipei, Taiwan. Professor Su received his Ph.D. (1998) degrees from National Chiao Tung University in Mechanical Engineering. His research interests and activities at Taipei TECH include Bonding technology, Nanotechnology, Coating technology, design and manufacturing of thin film solar cell, development of fabricating processes in

vapor chamber as a thermal module in electronic thermal management.

Wei-Ting Kuo was a graduate student for master degree from National Taipei University of Science and Technology during this work.

Chen-Kang Huang is an associate professor. He earned his Ph.D. in Mechanical Engineering from the University of California at Berkeley in 2004. His current research interests include heat transfer with phase change, computational fluid dynamics, air cleaning, and precision agriculture.